

Real-Time Assessment of Voltage Stability Using Local Bus Measurements in Power Systems

Talha Enes GÜMÜŞ*, Mustafa TURAN, Mehmet Ali YALÇIN

Abstract: Real-time monitoring of power system voltage stability is an important issue. Simplicity is desired in real-time assessments. This research proposes a novel method for determining the power system's Thevenin equivalent circuit parameters and for online voltage stability status assessment using local bus data. The proposed method performs voltage stability analysis with less data. The validity of the approach is tested by simulation on various load buses of the IEEE 30 bus test system. Simulations show that the proposed approach can be used for online voltage stability monitoring in power systems.

Keywords: Thevenin equivalent; local bus measurement; voltage stability

1 INTRODUCTION

The ever-increasing energy demand in power systems increases the disruptive effects that may occur in the power system. For this reason, determining how close the instability limits are is becoming increasingly important. Real-time monitoring of voltage stability limits has become essential. It is possible to assess the stability status of power systems using different methods.

The most common method used in voltage stability assessment is power flow-based approaches [1-3]. With power flow analysis, voltage amplitude and angle values of the system buses, generator production values, and details of line losses are obtained. In addition, with the obtained results, PV and QV curves of the interested bus in the system can be drawn, and stability analysis can be performed [4, 5].

In recent years, new approaches have been developed in stability analysis with the development of phasor measurement units (PMUs). Synchronous data can be obtained from a large number of buses using PMUs. Voltage stability assessment can be made with this synchronously collected data [6, 7].

In addition, voltage stability analysis studies are carried out using Thevenin equivalent circuit in power systems [8]. Thevenin equivalent-based analyses aim to determine the critical values of the power system. The biggest problem in these studies is correctly estimating the equivalent circuit parameters. Approaches using the least squares technique [9] and inverse matrix solution-based estimations have been developed for estimating Thevenin equivalent circuit parameters [10-12]. Stability analysis can be performed by obtaining the Thevenin equivalent circuit parameters (E_{Th} , Z_{Th}) for the load bus k by performing power flow analysis [13, 14]. However, many local parameter measurements and matrix operations are required before each evaluation [15]. This situation does not give fast results because it requires a long process.

Recently, researchers have proposed various methods for finding the Thevenin equivalent of power systems. Among these, only those that use local bus parameters to find Thevenin equivalent circuit parameters are attractive due to their ease of use [16-18]. In these studies, the voltage stability of the bus is assessed using the maximum power transfer law, and the Thevenin equivalent circuit

parameters, as observed from the load bus k of the power system, are computed using local bus parameters.

In this study, the Thevenin voltage for the load bus k , whose stability is to be investigated, has been calculated analytically using only consecutive measurements made on the bus k . A new polynomial for the Thevenin impedance has been proposed, and the Thevenin impedance has been calculated using this polynomial. The voltage stability assessment of the load bus k has been performed in real-time using the calculated Thevenin equivalent circuit parameters. The proposed method has been validated by using simulations on the IEEE 30 bus test system [19], and the results have been compared with those obtained from the power flow-based approach. The results obtained from both methods have been observed to be close. This situation showed that the voltage stability analysis of the load bus k can be performed using only the local bus measurements without the need for all the system data used in the power flow analysis.

2 ESTIMATION OF THE THEVENIN EQUIVALENT CIRCUIT PARAMETERS

The multi-bus power system can be represented with a Thevenin equivalent circuit, which is a single-port circuit, and this scheme has been used in voltage stability studies [21]. In this approach, a Thevenin source and a Thevenin impedance in series symbolize the multi-bus power system. Fig. 1 shows the Multi-bus power system and its Thevenin Equivalent seen from load bus k .

The Kirchhoff loop expression for the equivalent circuit shown in Fig. 1 is given in phasor Eq. (1).

$$\dot{E}_{Th} = \dot{V}_k + \dot{Z}_{Th} \cdot \dot{I}_k \quad (1)$$

In order to see basic trigonometric relations, the phasor diagram of Eq. (1) is drawn in Fig. 2. By using the phasor diagram and additional alpha and beta axis projections, Eqs. (2) to (6) can easily be written from the ABC triangle.

$$E_{Th} = \sqrt{E_{Th\alpha}^2 + E_{Th\beta}^2} \quad ;$$

$$Z_{Th} = \sqrt{R_{Th}^2 + X_{Th}^2} \quad ; \quad \theta = \tan^{-1} \left(\frac{X_{Th}}{R_{Th}} \right) \quad (2)$$

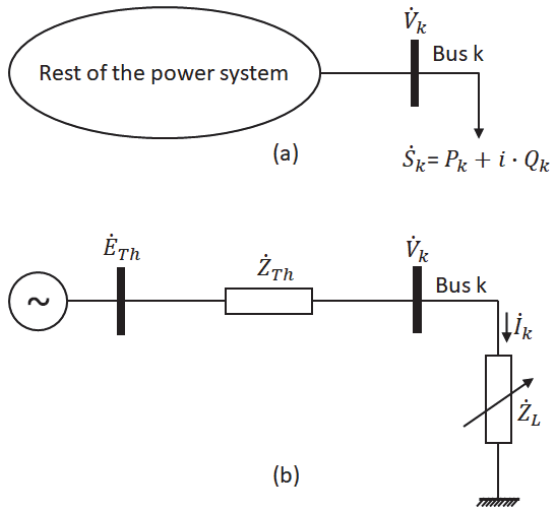


Figure 1 (a) Multi-bus power system and bus k (b) Thevenin equivalent circuit of power system seen from load bus k

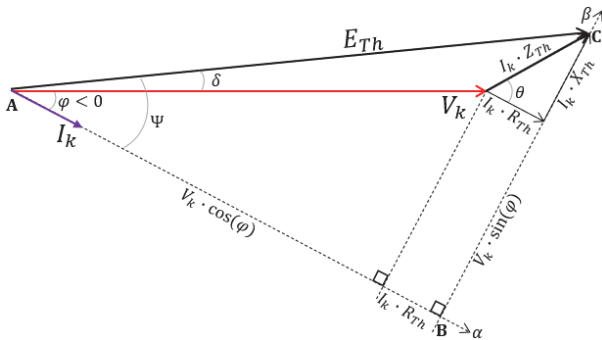


Figure 2 Thevenin equivalent circuit phasor diagram

$$\overline{AB} = E_{Th\alpha} = V_{k1} \cdot \cos(\varphi_1) + I_{k1} \cdot R_{Th} \quad (3)$$

$$\overline{BC} = E_{Th\beta} = V_{k1} \cdot \sin(\varphi_1) + I_{k1} \cdot X_{Th} \quad (4)$$

These two equations are insufficient for the four unknowns of the system. The number of equations can be increased to four by taking two consecutive measurements at the k^{th} bus. The obtained equation system can be given in matrix form with Eqs. (5) to (6).

$$[A] = \begin{bmatrix} 1 & 0 & -I_{k1} & 0 \\ 0 & 1 & 0 & -I_{k1} \\ 1 & 0 & -I_{k2} & 0 \\ 0 & 1 & 0 & -I_{k2} \end{bmatrix}; \quad (5)$$

$$[x] = \begin{bmatrix} E_{Th\alpha} \\ E_{Th\beta} \\ R_{Th} \\ X_{Th} \end{bmatrix}; [B] = \begin{bmatrix} V_{k1} \cdot \cos(\varphi_1) \\ V_{k1} \cdot \sin(\varphi_1) \\ V_{k2} \cdot \cos(\varphi_2) \\ V_{k2} \cdot \sin(\varphi_2) \end{bmatrix}$$

$$[A] \cdot [x] = [B]; [x] = [A]^{-1} \cdot [B] \quad (6)$$

After calculating the unknown vector $[x]$, the E_{Th} , Z_{Th} , and θ parameters are determined using the vector components given in Eq. (2).

In a power system with sufficient active and reactive power reserves, the magnitude of E_{Th} can be assumed

constant in a short time window. However, infinite sets of Z_{Th} and θ satisfy the voltage, current, and power values at the k^{th} bus of the power system for constant E_{Th} . Therefore, E_{Th} is accurately estimated, while Z_{Th} and θ take pseudo values that satisfy the equations, not real ones. This is valid for the cases where the components $E_{Th\alpha}$ and $E_{Th\beta}$ vary between two consecutive measurements. If these components remain constant, all variables in the matrix solution will be calculated correctly. In addition to finding E_{Th} with great accuracy from the matrix solution, additional approaches are required to estimate the Z_{Th} and θ parameters correctly. Applying the Pythagorean Theorem to the ABC triangle given in Fig. 2, Eq. (7) is obtained.

$$E_{Th}^2 = (V_k \cdot \cos\varphi_k + I_k \cdot R_{Th})^2 + (V_k \cdot \sin\varphi_k + I_k \cdot X_{Th})^2 \quad (7)$$

By substituting $R_{Th} = Z_{Th} \cdot \cos(\theta)$ and $X_{Th} = Z_{Th} \cdot \sin(\theta)$ in Eq. (7), the polynomial given in Eq. (8) can be written.

$$I_k^2 \cdot Z_{Th}^2 + (2 \cdot V_k \cdot I_k \cdot \cos(\theta + \varphi_k)) \cdot Z_{Th} + (V_k^2 - E_{Th}^2) = 0 \quad (8)$$

The characteristic impedance angle θ increases in energy transmission lines as the voltage level increases. It is known that this angle takes a value between 70° - 90° in transmission lines [21, 22]. In this study, the angle θ is taken as 80° . Thus, the E_{Th} estimated from the matrix solution in Eq. (6), the voltage-current - power angle of the k^{th} bus, and the angle θ are written in Eq. (8), and the positive root is taken to determine the Z_{Th} value. The load angle δ to be used in the stability analysis is determined by Eq. (9) obtained using the phasor diagram and trigonometric relations given in Fig. 2.

$$\delta = a \cos\left(\frac{E_{Th}^2 - I_k^2 \cdot Z_{Th}^2 + V_k^2}{2 \cdot E_{Th} \cdot V_k}\right) \quad (9)$$

Thus, all the Thevenin equivalent circuit parameters of the power system, as seen from the k^{th} bus, are attained. Those estimated parameters and application of maximum power transfer principles will allow easy assessment of voltage stability limits.

3 CRITICAL VOLTAGE AND VOLTAGE STABILITY MARGIN

The maximum apparent power transfer occurs when the magnitude of the Thevenin equivalent circuit impedance for the k bus, where the stability analysis will be performed in the power system, is equal to the load impedance. At the moment of maximum power transfer, the critical current is drawn from the load bus.

$$Z_L \cdot I_{k,cr} = Z_{Th} \cdot I_{k,cr} \quad (10)$$

The Equation for maximum power transfer is given in Eq. (10). The phasor diagram for Eq. (10) is shown in Fig. 3.

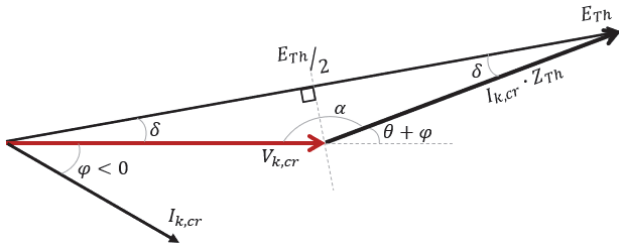


Figure 3 Phasor diagram at maximum power transfer

From the phasor diagram given in Fig. 3, the critical voltage for the k^{th} bus is obtained in Eq. 11 [23].

$$V_{k,cr} = \frac{E_{Th}}{2 \cdot \cos(\delta)} \quad (11)$$

Using the critical voltage and bus voltage in the voltage stability margin expression of the load bus k given in Eq. (12) [24], the voltage stability status of the k^{th} bus can be monitored in real-time.

$$VSM_V = \frac{V_k - V_{k,cr}}{V_{k,cr}} \quad (12)$$

The examined bus's voltage stability margin, or VSM_V , has a value between 0 and 1, and as it gets closer to 0, the bus becomes closer to the instability limit. The flowchart of the proposed approach is given in Fig. 4. Details of the steps of the proposed approach are given in the flowchart. If VSM_V is under alarm level, some precautionary measures, such as load shedding, can be initiated.

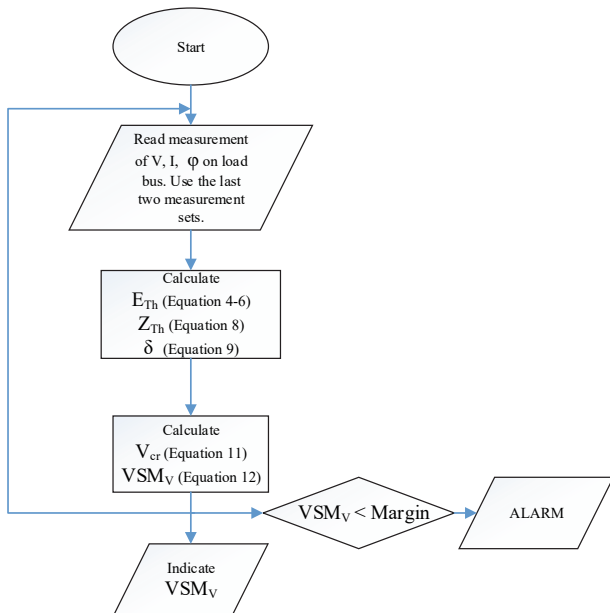


Figure 4 Flowchart of proposed approach

4 SIMULATIONS

The proposed method has been applied to different load buses of the IEEE 30 bus test system for validation. The power of the load bus was increased step by step until the maximum power point was reached, keeping the power factor constant. Current, voltage, and power factor measurements have been taken on the load bus k . Using the

proposed approach and the successive measurements taken from the load bus k , the Thevenin equivalent circuit parameters for the load bus k have been computed. Then, the critical voltage for the load bus k has been calculated using the Thevenin equivalent circuit parameters. The voltage stability margin of the bus has been calculated in real-time using the critical voltage estimation and bus voltage. The critical voltage and bus voltage for the 7th load bus of the test system were calculated in real-time, and the results are given in Fig. 4. The point where the bus voltage and critical voltage intersect in Fig. 4 shows the critical point of the system in terms of voltage stability. S_{Max} , indicated by a dashed line in Fig. 4, shows the maximum power limit that can be drawn from the bus with load flow analysis. It is seen that the calculated critical point and the maximum power that can be drawn from the bus using power flow analysis are quite close to each other.

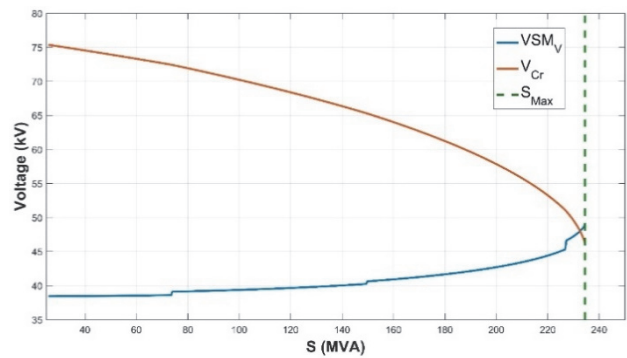


Figure 4 Critical voltage and bus voltage of the 7th bus of IEEE 30 bus test system

Using the calculated critical voltage and bus voltage, the voltage stability margin VSM_V of the bus was calculated, and the results are given graphically in Fig. 5. Fig. 5 shows that at the point where the voltage stability margin is zero, the maximum power value from the bus and the stability margin are very close to each other. This situation indicates that the critical points calculated using the power flow analysis and those estimated using the proposed method are very close.

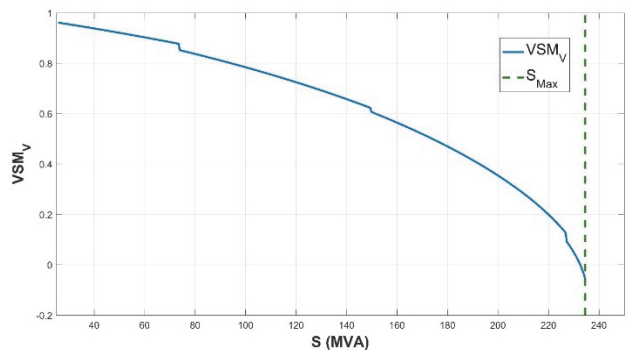


Figure 5 VSM_V for the 7th bus of IEEE 30 bus test system

The critical voltage and bus voltage of load bus number 12 are given in Fig. 6. It is seen that the intersection point of the critical voltage value and bus voltage calculated using the Thevenin equivalent are very close to the maximum power point calculated with the power flow analysis.

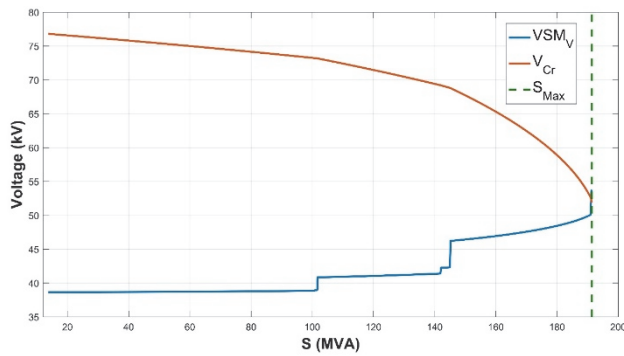


Figure 6 Critical voltage and bus voltage of the 12nd bus of IEEE 30 bus test system

In Fig. 7, the voltage stability margin of load bus number 12 is given.

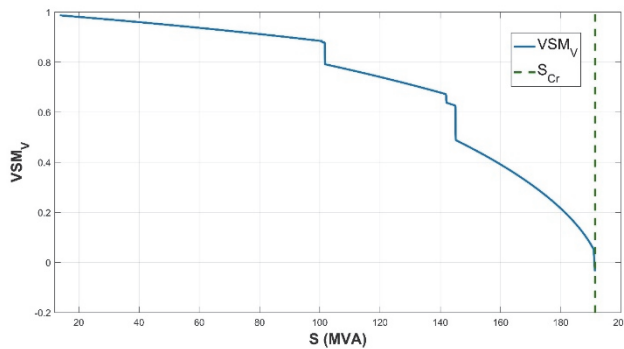


Figure 7 VSM_V for the 12nd bus of IEEE 30 bus test system

In Fig. 8, the critical voltage and bus voltage of load bus number 21 are given.

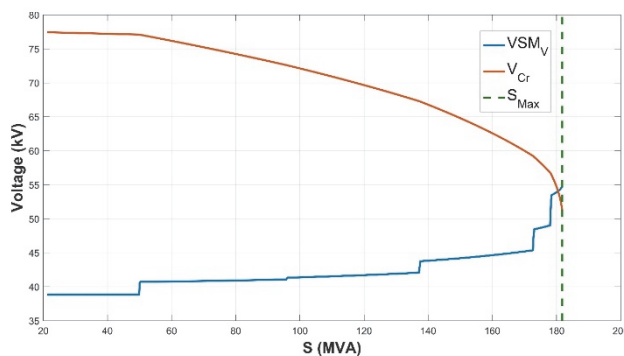


Figure 8 Critical voltage and bus voltage of the 21st bus of IEEE 30 bus test system

In Fig. 9, the voltage stability margin of load bus number 21 is given.

It is seen that the voltage stability margin calculated for different load buses of the test system and the maximum power point calculated with power flow analysis are quite close to each other. This situation shows the validity of the proposed method. It allows the assessment of the voltage stability of the load bus k with only local bus measurements without the need for power flow analysis. The proposed method also provides information about the generators in the system that have reached their reactive power limits. The sudden step-shaped changes in the voltage stability margin calculated for different load buses of the test system are due to the generators reaching their reactive power limits. The S_{Max} in the graphs given for different load buses

is the critical power value of the related bus obtained by the power flow analysis. It is seen that the results obtained from the power flow analysis and the results estimated with the proposed method are close to each other.

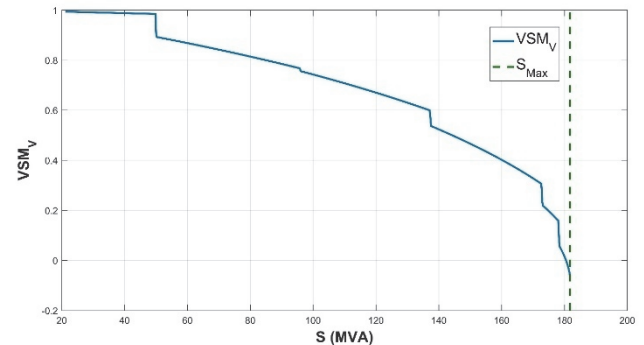


Figure 9 VSM_V for the 21st bus of IEEE 30 bus test system

Table 1 Proposed and compared power flow results

Bus Number	Proposed VSM_V	Power Flow VSM_V	Proposed Critical Power	Power flow Critical Power
7 th	0.0016	0	232.5 MVA	234.5 MVA
12 nd	-0.0017	0	191.1 MVA	191.4 MVA
21 st	0.0051	0	180.5 MVA	181.8 MVA

Tab. 1 shows the comparative results of the proposed method and the power flow. It can be seen that the VSM_V error between the proposed method and load flow analysis is less than 0.5%, proving the validity of the proposed method.

5 CONCLUSION

In this study, Thevenin equivalent circuit parameters for the load bus k have been calculated using local bus parameters. Using the calculated equivalent circuit parameters, the steady state voltage stability limit of the load bus k regarding the maximum power transfer law has been assessed.

The Thevenin Equivalent circuit for the bus to be analyzed for voltage stability has been calculated using only local bus measurements (load current, bus voltage, and load power factor). With the estimated equivalent circuit parameters, the critical voltage values of the load bus k have been calculated in real-time, the voltage stability margin (VSM_V) of the bus has been calculated using the calculated critical voltage values and bus voltages, and the voltage stability assessment of the load bus k has been achieved successfully. The proposed method offers ease of operation and the opportunity to obtain fast results since it uses only local bus measurements with a small amount of data.

With the proposed real-time monitoring, rapid information support can be provided for decisions such as load shedding from the system and fast commissioning of reactive power sources when necessary. It is recommended that the VSM_V alarm level be set at around 0.5 so that immediate precautions can be taken.

6 REFERENCES

- [1] Pourbagher, R., Derakhshandeh, S. Y., & Hamedani Golshan, M. E. (2022). An adaptive multi-step Levenberg-

- Marquardt continuation power flow method for voltage stability assessment in the III-conditioned power systems. *International Journal of Electrical Power and Energy Systems*, 134(January 2021), 107425. <https://doi.org/10.1016/j.ijepes.2021.107425>
- [2] Veerasamy, V., Abdul Wahab, N. I., Ramachandran, R., Othman, M. L., Hizam, H., Devendran, V. S., Irudayaraj, A. X. R., & Vinayagam, A. (2021). Recurrent network based power flow solution for voltage stability assessment and improvement with distributed energy sources. *Applied Energy*, 302(February), 117524. <https://doi.org/10.1016/j.apenergy.2021.117524>
- [3] Lai, Q., Liu, C., & Sun, K. (2021). Vulnerability assessment for voltage stability based on solvability regions of decoupled power flow equations. *Applied Energy*, 304(August), 117738. <https://doi.org/10.1016/j.apenergy.2021.117738>
- [4] Parihar, M., Bhaskar, M. K., Sarvate, D., Jain, D., & Bohra, D. (2018). *Analysis of Power Flow In IEEE Five Bus Power System Based on PV Curve Assessment, April*.
- [5] Parihar, M. (2017). Voltage Stability Analysis of Power System using Power World Simulator. *International Journal for Research in Applied Science and Engineering Technology*, V(XI), 2508-2515. <https://doi.org/10.22214/ijraset.2017.11351>
- [6] Glavic, M. & Van Cutsem, T. (2009). Wide-area detection of voltage instability from synchronized phasor measurements. Part II: Simulation Results. *IEEE Transactions on Power Systems*, 24(3), 1417-1425. <https://doi.org/10.1109/TPWRS.2009.2023272>
- [7] Glavic, M. & Van Cutsem, T. (2008). Detecting with PMUs the onset of voltage instability caused by a large disturbance. *IEEE Power and Energy Society 2008 General Meeting: Conversion and Delivery of Electrical Energy in the 21st Century, PES, June*. <https://doi.org/10.1109/PES.2008.4596308>
- [8] Bidadfar, A., Hooshyar, H., & Vanfretti, L. (2018). Dynamic Thévenin equivalent and reduced network models for PMU-based power system voltage stability analysis. *Sustainable Energy, Grids and Networks*, 16, 126-135. <https://doi.org/10.1016/j.segan.2018.07.002>
- [9] Milđević, B. & Begović, M. (2003). Voltage-stability protection and control using a wide-area network of phasor measurements. *IEEE Transactions on Power Systems*, 18(1), 121-127. <https://doi.org/10.1109/TPWRS.2002.805018>
- [10] Haque, M. H. (2003). On-line monitoring of maximum permissible loading of a power system within voltage stability limits. *IEE Proceedings on Generation, Transmission and Distribution*, 150(1). <https://doi.org/10.1093/oxfordjournals.ndt.a091183>
- [11] Osipov, D., Ferreira, A. P. F., Chow, J. H., Taranto, G. N., & Assis, T. M. L. (2022a). Application of Thévenin equivalent sensitivity equations for reliable voltage stability assessment. *Electric Power Systems Research*, 211(October 2021), 108424. <https://doi.org/10.1016/j.epr.2022.108424>
- [12] Sobhy, A., Saeed, M. A., Eladl, A. A., & Abdelkader, S. M. (2022). Online estimation of thévenin equivalent using discrete fourier transform. *Electric Power Systems Research*, 205(December 2021), 107772. <https://doi.org/10.1016/j.epr.2022.107772>
- [13] Ratra, S., Tiwari, R., & Niazi, K. R. (2018). Voltage stability assessment in power systems using line voltage stability index. *Computers and Electrical Engineering*, 70, 199-211. <https://doi.org/10.1016/j.compeleceng.2017.12.046>
- [14] Yang, J. & Yun, Z. (2020). The Thévenin equivalent based power flow method for integrated transmission and radial distribution networks. *International Journal of Electrical Power and Energy Systems*, 123(June), 106294. <https://doi.org/10.1016/j.ijepes.2020.106294>
- [15] Ferreira, A. P. F., Osipov, D., Taranto, G. N., Assis, T. M. L., & Chow, J. H. (2023). Extended real-time voltage instability identification method based on synchronized phasor measurements. *International Journal of Electrical Power and Energy Systems*, 147(November 2022), 108804. <https://doi.org/10.1016/j.ijepes.2022.108804>
- [16] Hu, F., Sun, K., Del Rosso, A., Farantatos, E., & Bhatt, N. (2016). Measurement-Based Real-Time Voltage Stability Monitoring for Load Areas. *IEEE Transactions on Power Systems*, 31(4), 2787-2798. <https://doi.org/10.1109/TPWRS.2015.2477080>
- [17] Shakerighadi, B., Aminifar, F., & Afsharnia, S. (2015). A real-time voltage stability index based on local measurements. *2015 23rd Iranian Conference on Electrical Engineering*, 1492-1497. <https://doi.org/10.1109/IranianCEE.2015.7146456>
- [18] Tobón V., J. E., Gutiérrez, R. E. C., & Ramirez, J. M. (2014). 27-Voltage collapse detection based on local measurements. *Electric Power Systems Research*, 107, 77-84. <https://doi.org/10.1016/j.epr.2013.09.013>
- [19] IEEE. (n.d.). *IEEE 30 Bus Test System*. From https://labs.ece.uw.edu/pstca/pf30/pg_tca30bus.htm
- [20] Zhou, X., Liu, Y., Chang, P., Xue, F., & Zhang, T. (2022). Voltage Stability Analysis of a Power System with Wind Power Based on the Thévenin Equivalent Analytical Method. *Electronics (Switzerland)*, 11(11), 1-20. <https://doi.org/10.3390/electronics11111758>
- [21] Brusilowicz, B., Rebizant, W., & Szafran, J. (2011). A new method of voltage stability margin estimation based on local measurements. *2011 International Conference on Advanced Power System Automation and Protection*, 2443-2447. <https://doi.org/10.1109/APAP.2011.6180655>
- [22] Birchfield, A., Schweitzer, E., Athari, M., Xu, T., Overbye, T., Scaglione, A., & Wang, Z. (2017). A Metric-Based Validation Process to Assess the Realism of Synthetic Power Grids. *Energies*, 10(8), 1233. <https://doi.org/10.3390/en10081233>
- [23] Hussain, M., Sultan, M., Uzma, F., Longsheng, C., Malik, M. Y., Butt, A. R., Sajjad, A., Younis, I., & Imran, M. (2022). A comparative analysis of renewable and non-renewable energy generation to relegate CO₂ emissions and general costs in household systems. *Environmental Science and Pollution Research*, 29(52), 78795-78808. <https://doi.org/10.1007/s11356-022-21121-0>
- [24] Canizares, C. A., De Souza, A. C. Z., & Quintana, V. H. (1996). Comparison of performance indices for detection of proximity to voltage collapse. *IEEE Transactions on Power Systems*, 11(3), 1441-1450. <https://doi.org/10.1109/59.535685>

Contact information:

Talha Enes GÜMÜŞ, PhD, Assistant Professor
(Corresponding author)
Department of Electrical and Electronics Engineering,
Engineering Faculty Sakarya University,
54187, Serdivan, Sakarya, Turkey
E-mail: tgumus@sakarya.edu.tr

Mustafa TURAN, PhD, Assistant Professor
Department of Electrical and Electronics Engineering,
Engineering Faculty Sakarya University,
54187, Serdivan, Sakarya, Turkey
E-mail: turan@sakarya.edu.tr

Mehmet Ali YALÇIN, PhD, Professor,
Department of Electrical and Electronics Engineering,
Engineering Faculty Sakarya University,
54187, Serdivan, Sakarya, Turkey
E-mail: yalcin@sakarya.edu.tr